

## *In vitro* Evaluation of Aldoxime Interactions with Human Acetylcholinesterase

Zrinka Kovarik,<sup>a,\*</sup> Maja Čalić,<sup>a</sup> Anita Bosak,<sup>a</sup> Goran Šinko,<sup>a</sup> and Dubravko Jelić<sup>b</sup>

<sup>a</sup>Institute for Medical Research and Occupational Health, P. O. Box 291, HR-10001 Zagreb, Croatia

<sup>b</sup>GlaxoSmithKline Research Center Zagreb, Prilaz Baruna Filipovića 29, HR-10000 Zagreb, Croatia

RECEIVED APRIL 3, 2007; REVISED MAY 28, 2007; ACCEPTED JUNE 4, 2007

*Keywords*  
cytotoxicity  
nerve agents  
oxime  
phosphorylation  
protection  
reactivation

We related the ability of eleven pyridinium and imidazolium aldoximes to reactivate tabun-inhibited human erythrocyte acetylcholinesterase with their molecular properties. Using molecular mechanics we performed conformational analysis to determine the flexibility of the aldoximes. Semi-empirical calculations show that differences in reactivation rates probably do not origin from different electron density on the oxygen of the oxime group, but can be explained by the steric hindrance within the aldoxime molecule. Tabun-inhibited acetylcholinesterase was efficiently reactivated by flexible bispyridinium *para*-aldoximes with propylene or butylene linker. Although pyridinium/imidazolium aldoximes with the oxime group in *ortho*-position did not show significant reactivation ability, they protected acetylcholinesterase against phosphorylation by tabun due to their high affinity for the native acetylcholinesterase. The aldoximes were examined for cytotoxicity on different cell lines and no cytotoxic effect was observed for doses of up to 400  $\mu\text{mol dm}^{-3}$ .

### INTRODUCTION

The availability of highly toxic organophosphorus compounds (OP), such as nerve agents, underlines the necessity for an effective medical treatment. Acute OP toxicity is primarily caused by the inhibition of acetylcholinesterase (AChE; EC 3.1.1.7) via phosphorylation of the enzyme catalytic site.<sup>1</sup> Reactivators of inhibited AChE, such as aldoximes, are a mainstay of the treatment.<sup>2</sup> However, the commercially available aldoxime, 2-PAM, is considered to be rather ineffective against various nerve agents, *e.g.* tabun.<sup>3</sup> This led to the synthesis and investigation of numerous aldoximes in the past decades.<sup>2,4–6</sup> TMB-4 is one of the classical aldoximes and an

effective reactivator of AChE phosphorylated by tabun.<sup>3,6</sup> Our recent reactivation studies with pyridinium aldoximes, which are similar to TMB-4 with the *para*-positioned oxime group, gave promising results in reactivating tabun-phosphorylated AChE and in the therapy of tabun-poisoning in mice.<sup>7,8</sup>

In this paper we bring together our previous results and the results of our *in vitro* study on aldoximes, shown in Figure 1, with the aim to relate the molecular properties of each aldoxime to its reactivation potency. To this end, we performed the conformational analysis of the aldoximes and determined the reactivation rate constants of human erythrocyte AChE inhibited by tabun. We also determined aldoxime protective potency against AChE

\* Author to whom correspondence should be addressed. (E-mail: zkovarik@imi.hr)

inhibition by tabun because in addition to acting as reactivators, aldoximes are also reversible inhibitors of AChE, and they protect the enzyme catalytic site against phosphorylation due to direct competition between them and the phosphorylating agent for binding to the enzyme's active site.<sup>9,10</sup> When we obtained promising results, we tested the cytotoxicity of the aldoximes on a defined set of cell lines. This kind of screening in the early stage of antidote development is a very important tool that can point out possible toxic effects of what appears as a promising compound, and can lead to structural optimization of an aldoxime.

## EXPERIMENTAL

### Chemicals

Aldoxime structures are given in Figure 1. HI-6 [1-(((4-carbamoylpyridinium-1-yl)methoxy)methyl)-2-((hydroxyimino)methyl)pyridinium chloride] was synthesized in the Department of Organic Chemistry, Faculty of Science, University of Zagreb, Croatia. TMB-4 [*N,N'*-(propano)bis(4-hydroxyiminomethyl)pyridinium bromide] was obtained from Borsnlijek, Sarajevo, Bosnia and Herzegovina. DMB-4 [*N,N'*-(ethano)bis(4-hydroxyiminomethyl)pyridinium methanesulphonate], MMB-4 [*N,N'*-(methano)bis(4-hydroxyiminomethyl)pyridinium chloride], HLö-7 [1-(((4-carbamoylpyridinium-1-yl)methoxy)methyl)-2-((hydroxyimino)methyl)-4-((hydroxyimino)methyl)pyridinium methanesulfonate], ICD-585 [1-(3-(4-carbamoylpyridinium-1-yl)propyl)-2-((hydroxyimino)methyl)pyridinium chloride], ICD-692 [4-carbamoyl-1-(3-(2-((hydroxyimino)methyl)-1-methyl-1*H*-imidazol-3-ium-3-yl)propyl)pyridinium chloride] and ICD-467 [2-((hydroxyimino)methyl)-1-methyl-3-((3-methyl-3-nitrobutan-2-yl)oxy)methyl)-1*H*-imidazol-3-ium chloride] were obtained from US Army Medical Research Institute of Chemical Defense, Aberdeen Proving Ground, MD, USA. K033 [1,4-bis(2-hydroxyiminomethylpyridinium) butane dibromide], K027 [1-1(4-hydroxyiminomethylpyridinium)-3-(4-carbamoylpyridinium) propane dibromide] and K048 [1-(4-hydroxyiminomethylpyridinium)-4-(4-carbamoylpyridinium) butane dibromide] were provided by Kamil Kuča, Faculty of Military Health Sciences, Hradec Kralove, Czech Republic. Tabun [ethyl *N,N*-dimethylphosphoramidocyanidate] was purchased from NC Laboratory, Spiez, Switzerland. Acetylthiocholine iodide (ATCh) and 5,5'-dithiobis(2-nitrobenzoic acid) (DTNB) were purchased from Sigma Chemical Co., St. Louis, MO, USA.

### Conformational Analysis of the Aldoximes

Conformational analysis was performed using MM2 and semi-empirical calculations with MOPAC 2000 software (PM-3 method with COSMO solvation model) created by J. J. P. Stewart (Fujitsu Ltd., Tokyo, Japan, 1999) according to published procedures.<sup>11,12</sup>

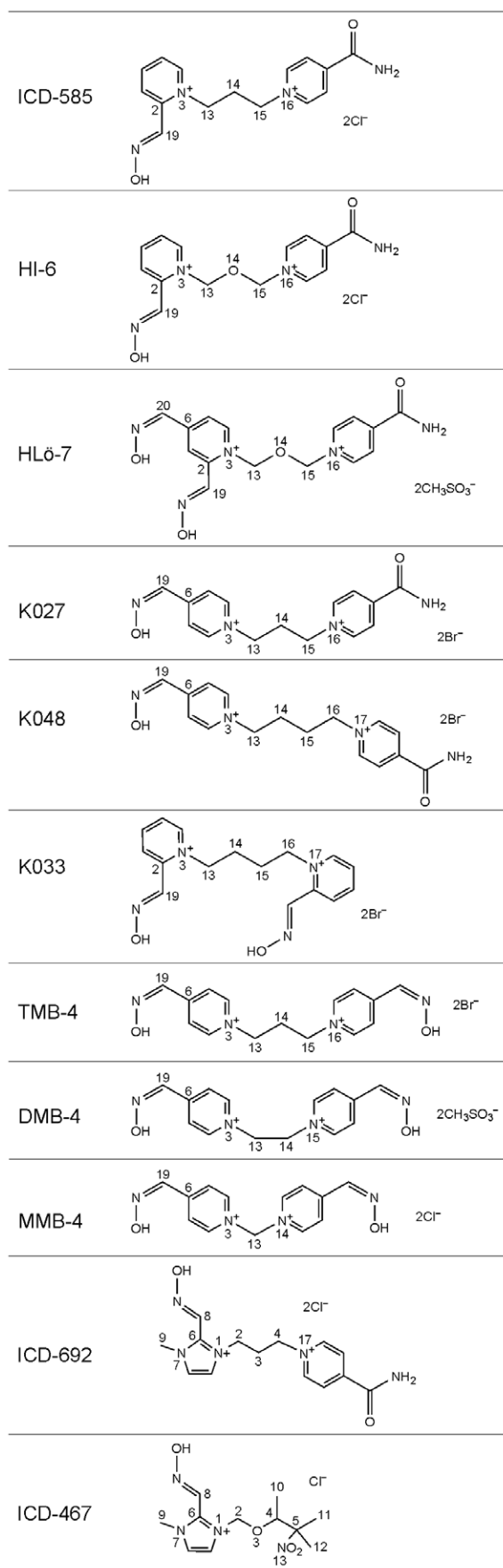


Figure 1. Structure of the aldoximes used in the study.

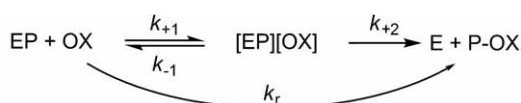
### AChE Activity Measurement

Native non-haemolysed human erythrocytes were the source of AChE; the final dilution during the enzyme assay was 400-fold. All experiments were done in 0.1 mol dm<sup>-3</sup> sodium phosphate buffer, pH = 7.4, at 25 °C. The enzyme activity was measured spectrophotometrically according to the Ellman procedure<sup>13</sup> with the thiol reagent DTNB (0.3 mmol dm<sup>-3</sup> final concentration) and ATCh as substrate. The increase in absorbance was read at 436 nm up to 2 min. All spectrophotometric measurements were performed on a CARY 300 spectrophotometer (Varian Inc., Australia).

### Reactivation of Tabun-inhibited AChE

Undiluted erythrocytes were incubated with 5 μmol dm<sup>-3</sup> tabun up to 60 min achieving 90–100 % inhibition. The incubation mixture was diluted 10 times with 0.1 mol dm<sup>-3</sup> phosphate buffer, pH = 7.4, containing the aldoxime to start reactivation. After a given time of reactivation aliquots were diluted 40 times, DTNB and ATCh (1.0 mmol dm<sup>-3</sup> final concentration) were added, and the enzyme activity was measured. An equivalent sample of uninhibited enzyme was diluted to the same extent as the inhibited AChE, and control activity was measured in the presence of aldoxime at concentrations used for reactivation. Both activities of control and reactivation mixture were corrected for oxime-induced hydrolysis of ATCh. No spontaneous reactivation of the phosphorylated enzyme took place.

Oxime-assisted reactivation of phosphorylated AChE proceeds according to Scheme 1:



Scheme 1.

where EP is the phosphorylated enzyme, [EP][OX] is the reversible Michaelis-type complex between EP and the aldoxime (OX), E is the active enzyme and P-OX the phosphorylated aldoxime,  $k_{+2}$  is the maximum first-order rate constant, and  $k_r$  is the overall second-order rate constant of reactivation. Scheme 1 is defined by the following equation:

$$\ln \frac{[\text{EP}]_0}{[\text{EP}]_t} = \frac{k_{+2} \cdot [\text{OX}]}{K_{\text{OX}} + [\text{OX}]} \cdot t = k_{\text{obs}} \cdot t \quad (1)$$

where [EP]<sub>0</sub> and [EP]<sub>t</sub> are concentrations of phosphorylated enzyme at time zero and at time *t*, respectively.  $K_{\text{OX}}$  is equal to the ratio  $(k_{-1} + k_{+2})/k_{+1}$ , and it approximates the dissociation constant of the [EP][OX] complex.  $k_{\text{obs}}$  is the observed first-order rate constant of reactivation at a given aldoxime concentration. The overall second-order rate constant of reactivation ( $k_r$ ) is the ratio

$$k_r = \frac{k_{+2}}{K_{\text{OX}}} \quad (2)$$

Experimental data were presented as reactivation

$$\text{Reactivation} / \% = \frac{v_{(\text{EP}+\text{OX})_t}}{v_{(\text{E}+\text{OX})_t}} \cdot 100 \quad (3)$$

where  $v_{(\text{EP}+\text{OX})_t}$  is activity of reactivated enzyme at time *t* and  $v_{(\text{E}+\text{OX})}$  stands for activity of enzyme incubated with aldoxime. Since  $(100 - \text{Reactivation}) / \%$  is equal to  $100 \cdot [\text{EP}]_t / [\text{EP}]_0$ , one can relate the experimental data to Eq. (1). At each aldoxime concentration,  $k_{\text{obs}}$  was calculated from the slope of the initial portion of  $\log [(100 - \text{Reactivation}) / \%]$  vs. time of reactivation. Reactivation with each aldoxime followed Eq. (1). Therefore,  $k_{+2}$  and  $K_{\text{OX}}$  were obtained by the non-linear fit of the relationship between  $k_{\text{obs}}$  vs. [OX], while  $k_r$  was calculated using Eq. (2).

### Reversible Inhibition of AChE

Reversible inhibition of AChE by aldoximes was measured in a medium which contained erythrocytes suspended in buffer, DTNB, the aldoxime and ATCh.

The inhibition constants were evaluated from the effect of substrate concentration on the degree of inhibition according to the equation:

$$K_{\text{app}} = \frac{v_i \cdot [\text{OX}]}{v_0 - v_i} = K_i + \frac{K_i}{K_s} \cdot [\text{S}] \quad (4)$$

$K_{\text{app}}$  is the apparent enzyme-aldoxime dissociation constant at a given substrate concentration [S], calculated from the enzyme activities  $v_0$  and  $v$  measured in the absence and in the presence of the aldoxime (OX), respectively.  $K_i$  is the enzyme-aldoxime dissociation constant of a complex formed in the catalytic site.  $K_s$  is the enzyme-substrate dissociation constant which should correspond to the Michaelis constant, if aldoxime binds only to the catalytic site.

### Protection of AChE against Phosphorylation

Protection of AChE against phosphorylation by tabun was measured in a medium which contained erythrocytes suspended in 0.1 mol dm<sup>-3</sup> phosphate buffer, DTNB, aldoxime, and tabun (100 nmol dm<sup>-3</sup>). After a given time of phosphorylation (up to 5 min) ATCh (1.0 mmol dm<sup>-3</sup> final concentration) was added and the increase in absorbance was read for 1 min. Control samples contained no aldoxime.

The second-order rate constant of inhibition by tabun ( $k_i$ ) was calculated from the equation:

$$\ln \frac{v_0}{v_{\text{OP}}} = k_i \cdot [\text{OP}] \cdot t \quad (5)$$

where  $v_{\text{OP}}$  and  $v_0$  are enzyme activities with and without tabun, respectively; [OP] is the concentration of tabun, and *t* is the time of inhibition. Protection was expressed in terms of the protective index (PI) which corresponds to the ratio:

$$\text{PI} = \frac{k_i}{k'_i} \quad (6)$$

The second-order rate constant of inhibition in the presence of aldoxime ( $k'_i$ ) was calculated using Eq. (5)

where  $v_0$  and  $v_{OP}$  denote enzyme activities in the absence of both aldoxime and tabun, and in their presence, respectively.

Protective indexes for all tested aldoximes were also determined theoretically from:

$$PI_{\text{theor}} = 1 + [OX]/K_i \quad (7)$$

where [OX] stands for aldoxime concentration, and  $K_i$  is the experimentally determined enzyme-aldoxime dissociation constant.

### *Oxime-catalysed Hydrolysis of Acetylthiocholine*

The reaction of ATCh with aldoxime was measured for 1 min in a medium which contained ATCh, aldoxime, DTNB and 0.1 mol dm<sup>-3</sup> phosphate buffer, pH = 7.4 at 25 °C. Two to four measurements were done with each ATCh/aldoxime concentration pair. The second-order rate constant of the non-enzymatic reaction ( $k_{NE}$ ) was calculated according to the following equation:

$$c/t = k_{NE} \cdot [S][OX] \quad (8)$$

where  $c$  is the released thiocholine concentration,  $t$  is the time of reaction, and [S] and [OX] are the initial ATCh and aldoxime concentrations, respectively. Thiocholine concentration was calculated from the absorbance monitored at 436 nm ( $\epsilon_M = 11\,000 \text{ dm}^3 \text{ mol}^{-1} \text{ cm}^{-1}$ ).<sup>14</sup>

### *Cell Lines*

Three malignant cell lines: human monocytic leukemia (THP-1, monocyte, ECACC-88081201),<sup>15</sup> human Caucasian hepatocyte carcinoma (Hep G2, epithelial, ECACC-85011430)<sup>16</sup> and Chinese Hamster Ovary cells (CHO, epithelial, ECACC-85050302)<sup>17</sup> were obtained from the European Collection of Cell Cultures, Great Britain. Human whole white blood cells (hWBC), isolated human polymorphonuclear cells (hPMN) and human peripheral blood mononuclear cells (hPMB) were prepared in GlaxoSmithKline Research Centre Zagreb Ltd., Croatia. Blood was obtained from the Transfusion Centre Zagreb, Croatia. All cells were maintained in completed RPMI 1640 medium (Institute of Immunology, Zagreb, Croatia) supplemented with 10 % Foetal Bovine Serum (BioWest, Nuille, France) at 37 °C in 5 % CO<sub>2</sub> atmosphere. Cells were passaged twice a week to be kept in a rapid-growth phase.

### *Cytotoxicity Assay*

Cells in the rapid-growth phase were exposed to the aldoximes. MTS reagent [3-(4,5-dimethylthiazole-2-yl)-2,5-diphenyl tetrazolium bromide] was used to measure the succinate dehydrogenase mitochondrial activity of living cells. This enzyme cuts the tetrazolium ring of MTS giving formazan that was determined spectrophotometrically at 490 nm.<sup>18</sup> Formazan develops only in the living and early apoptotic cells.

The aldoximes were examined for antiproliferative or cytotoxic effects following continuous exposure using the CellTiter 96® AQueous One Solution Cell Proliferation Assay (MTS Assay, Promega, USA). All aldoximes were prepared in DMSO as 10<sup>-2</sup> mol dm<sup>-3</sup> solutions, and added to the microtiter plate wells in the final concentrations of 800, 400, 200, 100, 50, 25, 12.5 and 6.25 μmol dm<sup>-3</sup>. Final dilution of DMSO did not exceed 1 %. The assay was performed on a defined set of different cell lines and each well contained 50 000 cells or 75 000 in the case of THP-1 cells. After cells were exposed to the aldoximes or 10 % DMSO as control for 24 h, 15 μL of MTS reagent (Promega, USA) was added to the cells cultured in microtiter plates. Absorbance was recorded with a spectrophotometric plate reader (Ultra, TECAN, USA). The method was programmed for TECAN robotic system in GEMINI pipetting software.<sup>19</sup> The results were expressed as OD values of non-treated cells and as IC<sub>50</sub> values.

## RESULTS AND DISCUSSION

Proper orientation in the active site gorge with the oxime group positioned towards the phosphorylated catalytic serine is one of the most important requirements for aldoximes that are being tested as reactivators of inhibited AChE.<sup>20,21</sup> Since the overall flexibility of the aldoxime molecule is a key property for achieving stabilisation in the vicinity of phosphorylated active site,<sup>22</sup> we performed the conformational analysis of the aldoximes (Figure 1) in order to relate their molecular properties to the studied AChE interactions. Table I shows the energy of aldoxime rotation bonds, while minimised aldoxime structures and the spatial arrangement of the oxime groups bonded to the pyridinium or imidazolium ring is presented in Figure 2. Generally, aldoximes with the oxime group in the *ortho*-position (ICD-585, HI-6, K033, ICD-692 and ICD-467) were less flexible than those with the oxime group in the *para*-position (K027, K048, TMB-4, DMB-4 and MMB-4) due to a higher rotation barrier of the N(3)-C(13) or N(1)-C(2) bond.<sup>23,24</sup> A higher rotation barrier in the *ortho*-aldoximes was caused by the steric hindrance of the linker connecting two rings, or in the case of ICD-467 the ring with the bulky aliphatic group. Although in MMB-4 oxime groups are *para*-positioned, the rotation barrier was higher than in other *para*-aldoximes due to a short linker.<sup>24</sup> Pyridinium rings of MMB-4 are stabilised in conformation with the angle of about 90° (Figure 2), and for their rotation additional energy is required. The rotation of a pyridinium ring carrying both *ortho*- and *para*-oxime groups, like in HLö-7, needs the same energy as in aldoximes with the *ortho*-positioned oxime group. Interestingly, the energy for the rotation of the oxime group (bond C(6)/C(2)-C(19)/C(20)) is the same regardless of its *ortho*- or *para*-position at the pyridinium ring, but is higher if the oxime group is *ortho*-positioned at the imidazolium ring.

TABLE I. Energy barriers ( $E$  / kcal mol<sup>-1</sup>) for rotation around single bonds in the aldoximes (N)<sup>(a), (b)</sup>

Aldoxime	$N$	Rotational bond	$E$	Rotational bond	$E$	Rotational bond	$E$	Rotational bond	$E$
ICD-585	5	N(3)–C(13)	14.9	C(2)–C(19)	5.5	C(13)–C(14)	30.4	C(15)–N(16)	1.2
						C(14)–C(15)	26.1		
HI-6	5	N(3)–C(13)	15.0	C(2)–C(19)	6.0	C(13)–O(14)	36.5	C(15)–N(16)	0.8
						O(14)–C(15)	34.0		
HLö-7	6	N(3)–C(13)	15.0	C(2)–C(19)	5.7	C(13)–O(14)	40.1	C(15)–N(16)	0.9
				C(6)–C(20)	6.4	O(14)–C(15)	8.3		
K027	5	N(3)–C(13)	0.7*	C(6)–C(19)	6.2	C(13)–C(14)	27.6		
		C(15)–N(16)				C(14)–C(15)	27.3		
K048	6	N(3)–C(13)	0.7*	C(6)–C(19)	6.2	C(13)–C(14)	27.6*		
		C(16)–N(17)				C(15)–C(16)			
						C(14)–C(15)	17.3		
K033	7	N(3)–C(13)	7.1*	C(2)–C(19)	5.0*	C(13)–C(14)	26.2*		
		C(16)–N(17)				C(15)–C(16)			
						C(14)–C(15)	31.1		
TMB-4	6	N(3)–C(13)	0.7*	C(6)–C(19)	6.2*	C(13)–C(14)	27.3*		
		C(15)–N(16)				C(14)–C(15)			
DMB-4	5	N(3)–C(13)	0.8*	C(6)–C(19)	6.2*	C(13)–C(14)	24.6		
		C(14)–N(15)							
MMB-4	4	N(3)–C(13)	3.3*	C(6)–C(19)	6.1*				
		C(13)–N(14)							
ICD-692	6	N(1)–C(2)	4.5	C(6)–C(8)	10.2	C(2)–C(3)	14.8	C(4)–N(5)	4.8
		N(7)–C(9)	1.7			C(3)–C(4)	16.8		
ICD-467	10	N(1)–C(2)	27.0	C(6)–C(8)	9.8	C(2)–O(3)	29.7	C(4)–C(5)	34.1
		N(7)–C(9)	0.4			O(3)–C(4)	66.3	C(5)–C(11)	3.2*
						C(4)–C(10)	3.4	C(5)–C(12)	
								C(5)–N(13)	41.6

<sup>(a)</sup> Energies were calculated using the MM2 method. <sup>(b)</sup> Asterisk denotes averaged value due to symmetry in the molecule.

TABLE II. Reactivation of tabun-inhibited human erythrocyte acetylcholinesterase by tested aldoximes<sup>(a), (b), (c)</sup>

Aldoxime ([OX]/mmol dm <sup>-3</sup> )	$k_{+2} \pm SE$ min <sup>-1</sup>	$K_{OX} \pm SE$ mmol dm <sup>-3</sup>	$k_r \pm SE$ dm <sup>3</sup> mol <sup>-1</sup> min <sup>-1</sup>	React <sub>max</sub> %	Time	Reference
ICD-585 (0.1–1.0)	ND	ND	ND	<15	24 h	this paper
HI-6 (0.1–1.0)	ND	ND	ND	10	24 h	7
HLö-7 (0.03–1)	0.008 ± 0.0005	0.047 ± 0.014	170 ± 51.8	80	8 h	this paper
K027 (0.03–5.0)	0.032 ± 0.002	0.085 ± 0.020	376 ± 92	100	2 h	7
K048 (0.05–5.0)	0.074 ± 0.003	0.11 ± 0.01	673 ± 67	100	30 min	7
K033 (0.1–1.0)	0.002 ± 0.0003	0.20 ± 0.10	10 ± 5	60	24 h	7
TMB-4 (0.05–10.0)	0.15 ± 0.02	0.49 ± 0.20	306 ± 131	100	20 min	7
DMB-4 (0.1–3.0)	0.002 ± 0.0001	0.048 ± 0.015	41.7 ± 13.2	70	16 h	24
MMB-4 (0.1–3.0)	0.004 ± 0.0004	0.28 ± 0.10	14.3 ± 5.3	80	10 h	24
ICD-692 (0.1–1.0)	ND	ND	ND	<15	24 h	this paper
ICD-467 (0.1–1.0)	ND	ND	ND	<15	24 h	this paper

<sup>(a)</sup> Constants (± standard errors) are calculated by Eqs. (1)–(3) from  $k_{obs}$  constants obtained in at least three experiments. <sup>(b)</sup> Maximum reactivation (React<sub>max</sub>) measured within the specified time of the experiment is also given. <sup>(c)</sup> ND = not determined.



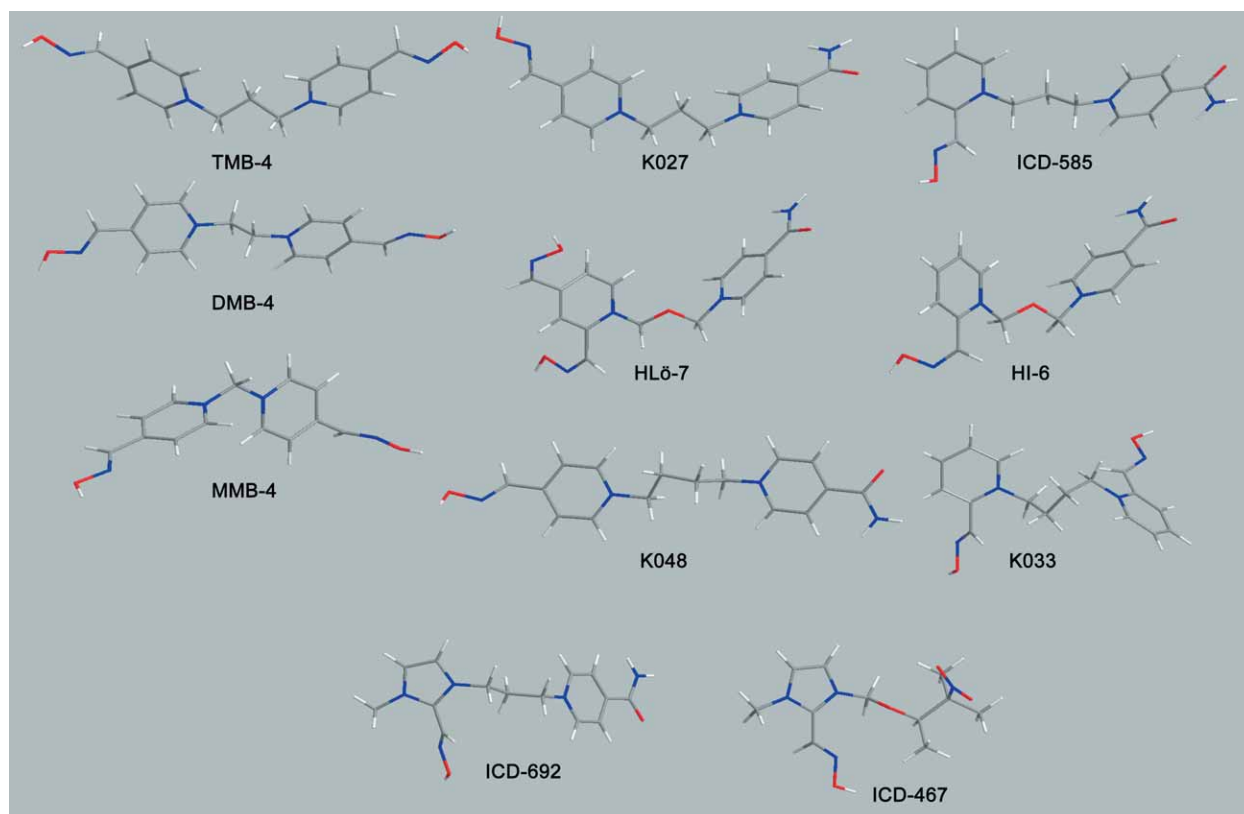


Figure 2. Minimised structures of the studied aldoximes. Presented atoms are carbon (dark grey), nitrogen (blue), oxygen (red). Hydrogen atoms are not shown for better visibility.

The highest rotation energy barriers observed for the bonds in the linker determined the overall aldoxime rigidity. Therefore, the most rigid aldoxime appeared to be the imidazolium aldoxime ICD-467 having the bulky 3-methyl-3-nitrobutane-2-yl group. Semi-empirical calculations also showed that the aldoximes had similar electron density for protonated oxygen ( $-0.35$ ) and for deprotonated oxygen ( $-0.89$ ) in the oxime group.

Table II shows the kinetic parameters for the reactivation of tabun-inhibited human AChE by the aldoximes, and one representative experiment is shown in Figure 3. Of all tested aldoximes two *para*-aldoximes, K048 and K027 had the highest reactivation potency for tabun-inhibited AChE because their relatively low concentrations were able to completely reactivate AChE in a short time.<sup>7</sup> Because of a fast first-order reactivation

TABLE III. Reversible inhibition of human erythrocyte acetylcholinesterase by tested aldoximes<sup>(a)</sup>

Aldoxime ([OX]/mmol dm <sup>-3</sup> )	[ATCh] / mmol dm <sup>-3</sup>	$K_i \pm SE$ / mmol dm <sup>-3</sup>	$K_s \pm SE$ / mmol dm <sup>-3</sup>	Reference
ICD-585 (0.010–0.080)	0.1–1.0	$0.028 \pm 0.002$	$0.88 \pm 0.12$	this paper
HI-6 (0.05–0.4)	0.1–5.0	0.031	–	35
HLö-7 (0.010–0.080)	0.1–1.0	$0.024 \pm 0.004$	$0.77 \pm 0.18$	this paper
K027 (0.064–0.45)	0.05–0.3	$0.073 \pm 0.01$	$0.13 \pm 0.02$	7
K048 (0.1–0.5)	0.05–1.0	$0.11 \pm 0.01$	$0.47 \pm 0.08$	7
K033 (0.01–0.2)	0.05–1.0	$0.017 \pm 0.002$	$0.79 \pm 0.22$	7
TMB-4 (0.1–0.7)	0.05–0.7	$0.18 \pm 0.01$	$0.96 \pm 0.16$	7
DMB-4 (0.05–0.50)	0.1–1.0	$0.10 \pm 0.02$	$0.74 \pm 0.19$	24
MMB-4 (0.25–0.70)	0.1–1.0	$0.49 \pm 0.07$	$0.48 \pm 0.09$	24
ICD-692 (0.010–0.040)	0.1–1.0	$0.018 \pm 0.001$	$7.8 \pm 16$	this paper
ICD-467 (0.005–0.010)	0.1–1.0	$0.0012 \pm 0.0001$	$1.4 \pm 0.4$	this paper

<sup>(a)</sup> Dissociation constants ( $\pm$  standard errors) were calculated using Eq. (4) from  $K_{app}$  obtained in at least three experiments.

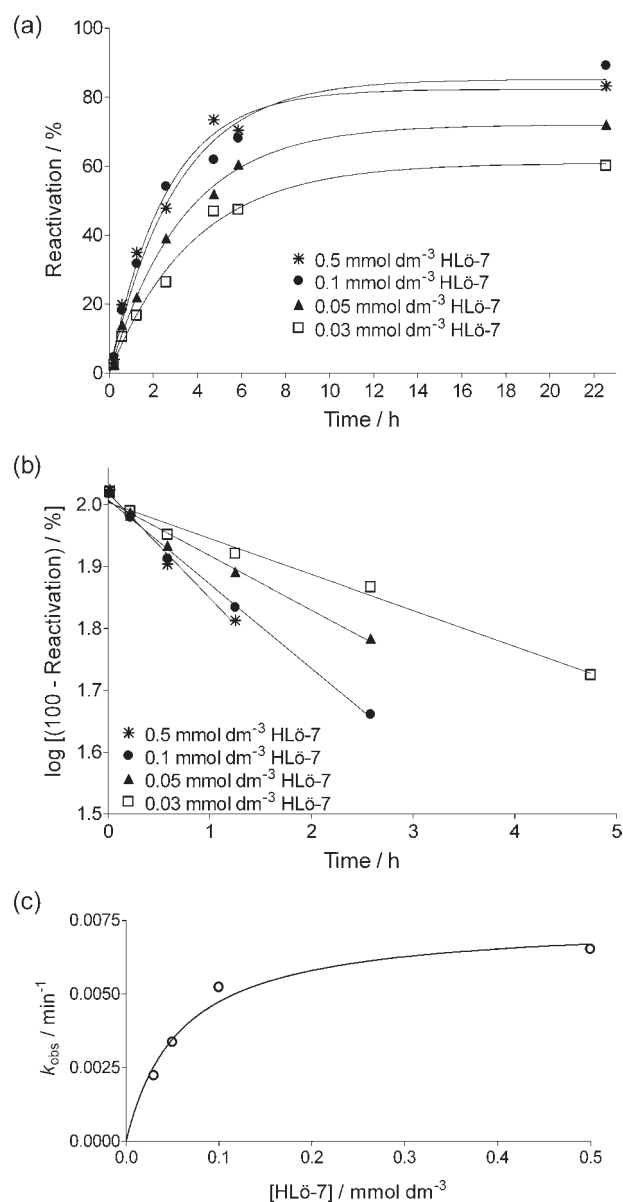


Figure 3. Reactivation of tabun-inhibited human erythrocyte AChE by HLö-7. (a) A single data point indicates calculated reactivation using Eq. (3). (b) Slopes of the reactivation curve yield  $k_{obs}$  constants. (c)  $k_{obs}$  is plotted as a function of HLö-7 and the curve is fitted using Eq. (1).

rate, TMB-4 also showed a significant reactivation potential.<sup>24</sup> Reactivation assisted by *ortho*-aldoximes was observed only with bispyridinium K033, reaching 60 % after 24 h. Maximum reactivation by other *ortho*-pyridinium aldoximes, ICD-585 and HI-6, and *ortho*-imidazolium aldoximes, ICD-692 and ICD-467, was lower than 15 %, and therefore their reactivation constants could not be determined. With HLö-7, a pyridinium aldoxime with both *ortho*- and *para*-positioned oxime groups on the pyridinium ring, enzyme activity was almost completely restored; primarily due to its high affinity for phosphorylated AChE (lower  $K_{OX}$ ; Table II). These results confirmed earlier studies with HLö-7.<sup>25,26</sup>

However, except for K027, K048 and TMB-4 no aldoxime showed complete reactivation, and the kinetics at the longer time intervals deviated from the first-order process described in Eq. (1). This deviation could be due to the post-inhibitory dealkylation of the phosphorylated enzyme known as aging.<sup>26</sup> It is known that the aging of tabun-inhibited human AChE is slow with the half-life of 13 h.<sup>27</sup> The other reason could be re-inhibition of the active enzyme by the phosphorylated aldoxime,<sup>21,28</sup> but no data on the inhibitory potency of conjugates of tabun and studied aldoximes is available in literature. However, conjugates of tabun and monopyridinium *para*-aldoxime 4-PAM or *ortho*-aldoxime 2-PAM were poor inhibitors of AChE, which was attributed to a combination of steric factors and a reduction in the electro-positivity of the phosphorus atom.<sup>29</sup> Therefore, aldoxime structure seemed to be the critical factor for tabun reactivation. It appears that, to reactivate tabun-inhibited AChE efficiently, the oxime group needs to be in the *para*-position on the pyridinium ring and the length of the linker between two rings should be three or four CH<sub>2</sub> groups. The type of the linker (propylene or oxapropylene) is less important. However, potent reactivators were also butylene-linked bisoximes that instead of pyridinium had imidazolium rings and the oxime group in the *ortho*-position.<sup>30</sup> Indeed, bispyridinium *para*-aldoximes with shorter linker than propylene and longer than butylene or monopyridinium *para*-aldoximes were not effective tabun-phosphorylated AChE reactivators.<sup>26,31,32</sup> A reactivation study of diisopropylphosphoryl-AChE showed that the most promising bispyridinium *para*-aldoxime was a propylene-linked bisaldoxime, while the most promising bispyridinium *ortho*-aldoxime was a heptylene-linked bisaldoxime.<sup>33</sup> The crystal structure of aldoxime-AChE complex explains different requirements of the chain length for reactivation; the most potent reactivators should span the active site of the phosphorylated AChE, and pyridinium rings should be stabilised by aromatic residues in the peripheral site and choline binding site of AChE.<sup>34</sup>

Since aldoximes are also reversible inhibitors of AChE, we determined dissociation constants of aldoxime-human erythrocyte AChE complex using Eq. (4) (Table III). The catalytic site of AChE showed the highest affinity (the lowest  $K_i$ ) for ICD-467, at least twenty times higher than that for the other aldoximes. The determined  $K_i$  constants were similar to constants published for other bispyridinium compounds.<sup>35</sup> However, the binding affinity of the aldoximes to the free enzyme mostly did not correlate with aldoxime efficacy in enzyme reactivation (*cf.* Table II). Therefore, if an aldoxime with a high binding affinity is stabilised far from the phosphorus atom, this aldoxime has a limited reactivation potency, which means that reactivation primarily depends on the displacement rate of the phosphorus

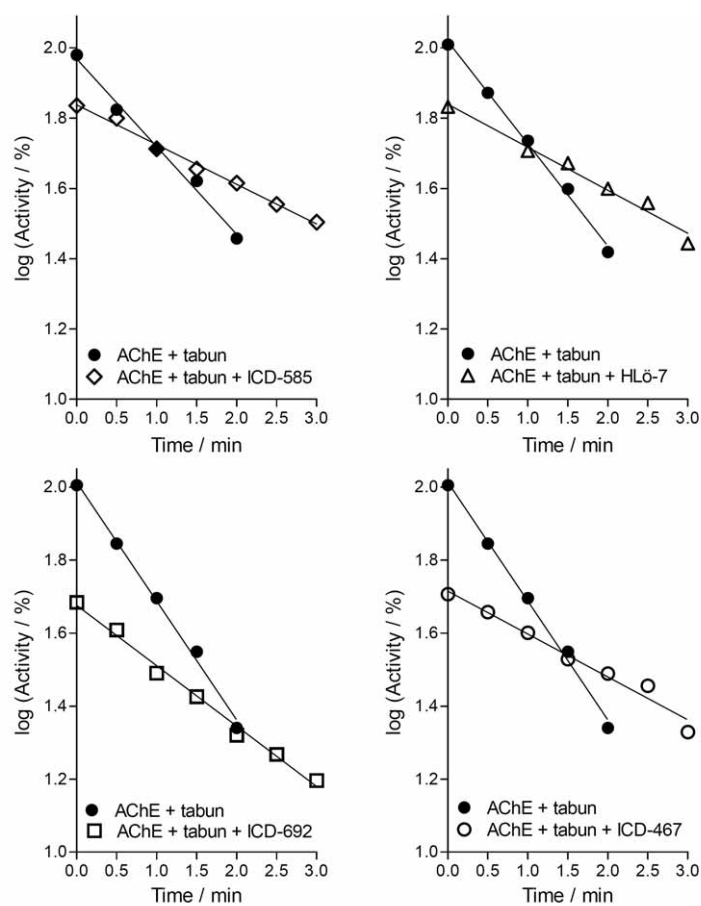


Figure 4. Progressive inhibition of AChE by tabun in the absence and in the presence of ICD-585, ICD-692, HLö-7 ( $20 \mu\text{mol dm}^{-3}$ ) and ICD-467 ( $2 \mu\text{mol dm}^{-3}$ ) wherefrom protective indexes were determined. Slopes represent the first-order inhibition rate constants.

moiety.<sup>36</sup> The  $K_s$  values, derived from the kinetics of inhibition with aldoximes were higher, but close to the previously determined  $K_M$ .<sup>37</sup> This supports our belief that the determined  $K_i$  constants correspond to the binding to the catalytic site of AChE. A higher  $K_s$  as well as its standard error for ICD-692 is probably due to an independence of  $K_{app}$  from substrate concentration, which

implies binding to the active site, but not to the catalytic site. However, higher substrate concentrations could not be used to determine possible aldoxime binding to the peripheral site of AChE because aldoximes reacted with acetylthiocholine and interfered with the enzyme assay.<sup>38–40</sup> The rate constants for aldoxime-catalysed hydrolysis of acetylthiocholine are given in Table IV. The

TABLE IV. Non-enzymatic reaction between the substrate acetylthiocholine (ATCh) and the aldoximes<sup>(a)</sup>

Aldoxime	[OX]/mmol dm <sup>-3</sup>	[ATCh] / mmol dm <sup>-3</sup>	$k_{NE} / \text{dm}^3 \text{mol}^{-1} \text{min}^{-1}$	Reference
ICD-585	0.01–0.08	0.1–1.0	$14.2 \pm 0.4$	this paper
HI-6	0.025–0.6	0.05–1.0	$10.7 \pm 0.1$	this paper
HLö-7	0.0025–0.08	0.1–1.0	$32.1 \pm 0.9$	this paper
K027	0.06–3.2	0.05–1.0	$12.0 \pm 0.4$	this paper
K048	0.1–3.0	0.05–1.0	$15.5 \pm 0.4$	this paper
K033	0.01–0.3	0.05–1.0	$25.6 \pm 0.9$	this paper
TMB-4	0.1–0.7	0.05–1.0	$31.0 \pm 0.5$	24
DMB-4	0.05–0.5	0.1–1.0	$29.3 \pm 1.0$	24
MMB-4	0.25–0.7	0.1–1.0	$32.0 \pm 1.0$	24
ICD-692	0.01–0.05	0.1–1.0	$13.7 \pm 0.4$	this paper
ICD-467	0.005–0.20	0.1–1.0	$17.2 \pm 0.7$	this paper

<sup>(a)</sup>Constants ( $\pm$  standard errors) were calculated in given concentration ranges using Eq. (8).



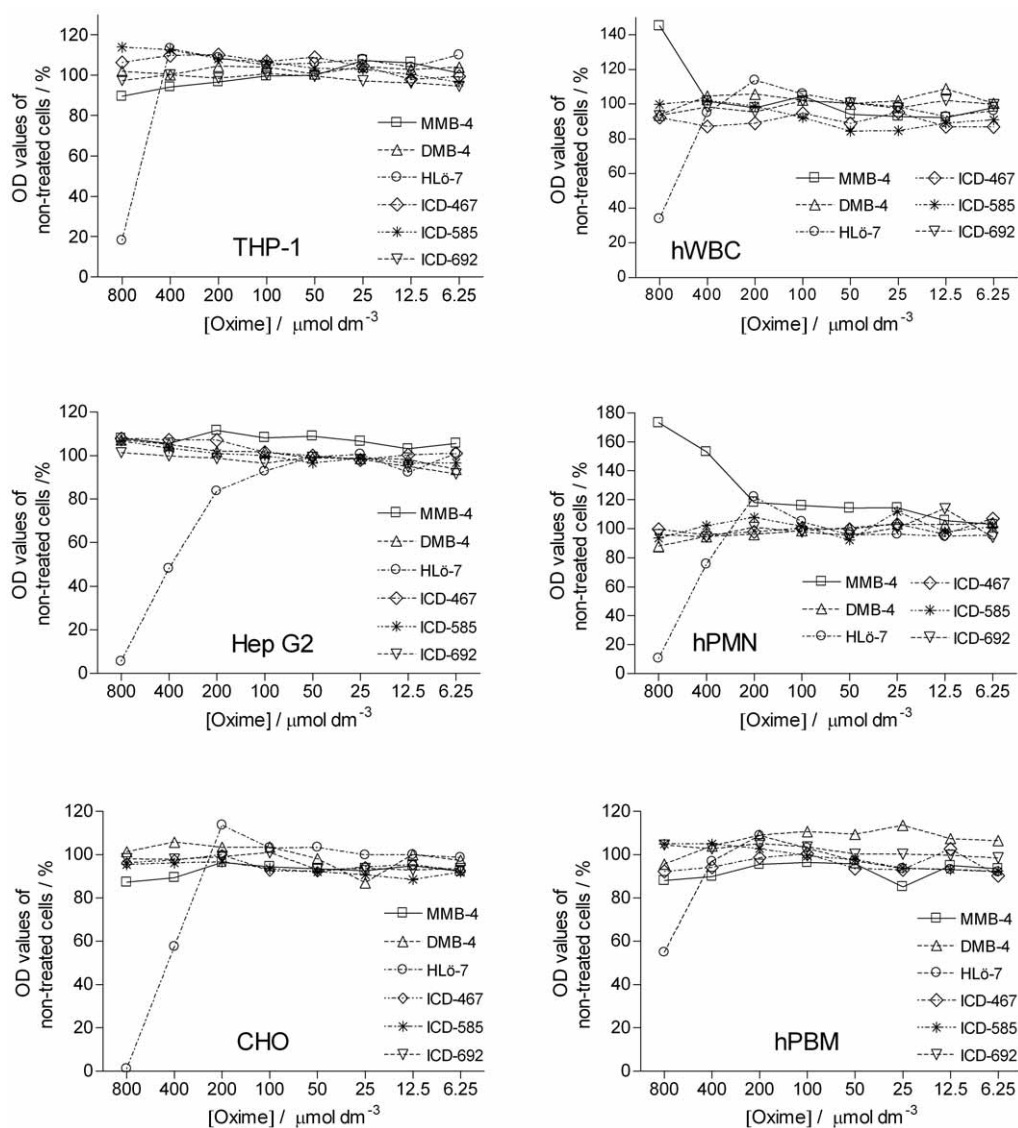


Figure 5. Cytotoxicity of the studied oximes on cell lines and human blood cells.

oxime group reacts with the AChE substrate acetylthiocholine on a 1:1 mole ratio basis, and thiocholine is one of the reaction products.<sup>23,41</sup> Therefore the rate of bisoximes is double that of monoximes. Constants were similar to the rate constant obtained for LüH6 (obidoxime), a bispyridinium aldoxime.<sup>35</sup>

As reversible inhibitors, aldoximes protect the catalytic serine against phosphorylation, which means that even though oxime-mediated reactivation is poor, aldoximes could be used as prophylactic agents.<sup>8,42</sup> We measured progressive inhibition of AChE by tabun in the absence and in the presence of aldoximes (Figure 4), and calculated protective indexes (PI; Table V). All tested aldoximes in concentrations corresponding to their  $K_i$  protected the enzyme from phosphorylation by tabun. A limited protection ability shown by ICD-692 and MMB-4 could be explained with lower concentrations

used than their  $K_i$ . The lower concentration for MMB-4 was intentional, because of its high  $K_i$ , but for ICD-692 it implies a deviation from the determined  $K_i$  as discussed in paragraph above. The protective index was also evaluated theoretically for all tested aldoximes. The relationship between experimentally and theoretically obtained protective indexes could be used to determine the aldoxime binding site in AChE.<sup>42</sup> Since experimentally determined PI corresponded to the theoretically obtained  $PI_{\text{theor}}$  using Eq. (7) (except for ICD-692), the aldoximes protected the enzyme primarily by binding to the catalytic site. As already mentioned, an additional study should provide a detailed mapping of the ICD-692 binding site in AChE.

Cytotoxicity screening was used to establish the basic cytotoxicity of the tested aldoximes. We used different cell lines, THP-1, Hep G2, CHO, as well as human

TABLE V. Protection with aldoximes (OX) against phosphorylation of human erythrocyte acetylcholinesterase by 100 nmol dm<sup>-3</sup> tabun<sup>(a)</sup>

Aldoxime	[OX]/mmol dm <sup>-3</sup>	PI	PI <sub>theor</sub>	Reference
ICD-585	0.02	1.9 ± 0.3	1.7	this paper
HI-6	0.03	2.2 ± 0.1	2.0	7
HLö-7	0.02	2.1 ± 0.2	1.8	this paper
K027	0.06	2.0 ± 0.1	1.9	7
K048	0.1	2.5 ± 0.3	1.9	7
K033	0.02	2.5 ± 0.3	2.2	7
TMB-4	0.2	2.6 ± 0.0	2.1	7
DMB-4	0.2	2.7 ± 0.4	3.0	24
MMB-4	0.2	1.5 ± 0.1	1.4	24
ICD-692	0.02	1.7 ± 0.3	2.1	this paper
ICD-467	0.002	2.7 ± 0.3	2.7	this paper

<sup>(a)</sup> Protective indexes (± standard deviation) are calculated using Eq. (6) from inhibition rate constants obtained in at least three experiments.

white blood cell types hWBC, hPMN and hPBM. The cytotoxic effect of tested aldoximes in 8 concentrations up to 0.8 mmol dm<sup>-3</sup> was evaluated by measuring the activity of mitochondrial succinate dehydrogenase of the living cells. Figure 5 shows dose-response curves expressed as the OD values of non-treated cells. Only HLö-7 showed a weak growth inhibition in most cell types, with the IC<sub>50</sub> ranging between 0.4 and 0.8 mmol dm<sup>-3</sup>. Since concentrations higher than 0.1 mmol dm<sup>-3</sup> are not suitable for human use,<sup>43</sup> observed cytotoxicity of HLö-7 does not limit further investigation of HLö-7. Interestingly, a stimulation of human polymorphonuclear cells was observed with MMB-4 after 24 hours, with the effect similar to the treatment of cells with 10 % DMSO. We did not observe a dose-response viability curve for other aldoximes for all cell types tested, which suggests that the aldoximes showed no cytotoxic effect in concentrations up to 0.8 mmol dm<sup>-3</sup> (IC<sub>50</sub> > 0.8 mmol dm<sup>-3</sup>). These results are in agreement with a previous cytotoxicity study on the same cell lines showing no cytotoxic effect of TMB-4, HI-6, K027, K033 and K048.<sup>7</sup>

## CONCLUSIONS

Pyridinium aldoximes with the oxime group in the *para*-position at the pyridinium ring were more flexible than those with the oxime group in the *ortho*-position at the pyridinium ring due to the lower rotation barrier of the N(3)–C(13) bond. All pyridinium aldoximes had the highest rotation barrier of the linker bonds ≈30 kcal mol<sup>-1</sup>. The most rigid aldoxime was the imidazolium aldoxime ICD-467, due to steric hindrance caused by the bulky 3-methyl-3-nitrobutane-2-yl group.

All bispyridinium aldoximes with the oxime group in the *para*-position were efficient reactivators of tabun-inhibited AChE; the most potent reactivator was K048, followed by K027, TMB-4, HLö-7, DMB-4 and

MMB-4. Five compounds with the oxime group in the *ortho*-position did not show significant reactivation potency for tabun-inhibited AChE.

All the aldoximes reversibly inhibited AChE and protected AChE against phosphorylation with tabun. The most potent inhibitors were the aldoximes with the oxime group in the *ortho*-position which did not show significant reactivation ability. Therefore, these oximes might be of interest as pre-treatment drugs due to their high affinity for the native AChE.

*Acknowledgements.* – We wish to thank Dr Irwin Klopovitz (US Army Medical Research Institute of Chemical Defense, Aberdeen Proving Ground, MD, USA) and Professor Palmer Taylor (University of California at San Diego, La Jolla, CA, USA) for supplying us with aldoximes ICD-585, HLö-7, MMB-4, DMB-4, ICD-692 and ICD-467. We also wish to thank Dr Kamil Kuča (Department of Toxicology, Faculty of Military Health Sciences, Hradec Králové, Czech Republic) for preparing and supplying the oximes K027, K033 and K048. This work was supported by the NATO Reintegration Grant (EAP.RIG.981791) and by the Croatian Ministry of Science, Education and Sports Grant (022–0222148–2889).

## REFERENCES

1. J. Bajgar, *Adv. Clin. Chem.* **38** (2004) 151–216.
2. A. P. Gray, *Drug. Metab. Rev.* **15** (1984) 557–589.
3. R. M. Dawson, *J. Appl. Toxicol.* **14** (1994) 317–331.
4. I. Primožič, R. Odžak, S. Tomić, V. Simeon-Rudolf, and E. Reiner, *J. Med. Chem. Def.* **2** (2004) 1–30.
5. E. Reiner and V. Simeon-Rudolf, *Arh. Hig. Rada Toksikol.* **57** (2006) 171–179.
6. M. P. Stojiljković and M. Jokanović, *Arh. Hig. Rada Toksikol.* **57** (2006) 435–443.
7. M. Čalić, A. Lucić Vrdoljak, B. Radić, D. Jelić, D. Jun, K. Kuča, and Z. Kovarik, *Toxicology* **219** (2006) 85–96.
8. A. Lucić Vrdoljak, M. Čalić, B. Radić, S. Berend, D. Jun, K. Kuča, and Z. Kovarik, *Toxicology* **228** (2006) 41–50.

9. V. Simeon-Rudolf, E. Reiner, M. Škrinjarić-Špoljar, B. Radić, A. Lucić, I. Primožič, and S. Tomić, *Arch. Toxicol.* **72** (1998) 289–295.
10. M. Škrinjarić-Špoljar, N. Burger, and J. Lovrić, *J. Enzym. Inhib.* **14** (1999) 331–341.
11. Z. Kovarik, A. Bosak, G. Šinko, and T. Latas, *Croat. Chem. Acta* **76** (2003) 63–67.
12. G. Šinko, A. Bosak, Z. Kovarik, and V. Simeon-Rudolf, *Chem.-Biol. Interact.* **157–158** (2005) 421–423.
13. G. L. Ellman, K. D. Courtney, V. Andres Jr., and R. M. Featherstone, *Biochem. Pharmacol.* **7** (1961) 88–95.
14. P. Eyer, F. Worek, D. Kiderlen, G. Šinko, A. Štuglin, V. Simeon-Rudolf, and E. Reiner, *Anal. Biochem.* **312** (2003) 224–227.
15. S. Tsuchiya, M. Yamabe, Y. Yamaguchi, Y. Kobayashi, T. Konno, and K. Tada, *Int. J. Cancer* **26** (1980) 171–176.
16. D. P. Aden, A. Fogel, S. Plotkin, I. Damjanov, and B. B. Knowles, *Nature* **282** (1979) 615–616.
17. T. Puck, S. Cieciora, and A. Robinson, *J. Exp. Med.* **108** (1958) 945–956.
18. T. Mosmann, *J. Immunol. Methods* **65** (1983) 55–63.
19. D. Verbanac, D. Jelić, V. Stepanić, I. Tatić, D. Žiher, and S. Koštrun, *Croat. Chem. Acta* **78** (2005) 133–139.
20. L. Wong, Z. Radić, R. J. Brüggemann, N. Hosea, H. A. Berman, and P. Taylor, *Biochemistry* **39** (2000) 5750–5757.
21. Z. Kovarik, Z. Radić, H. A. Berman, V. Simeon-Rudolf, E. Reiner, and P. Taylor, *Biochemistry* **43** (2004) 3222–3229.
22. K. Kuča, D. Jun and K. Musilek, *Mini-Rev. Med. Chem.* **6** (2006) 269–277.
23. G. Šinko, M. Čalić, and Z. Kovarik, *FEBS Lett.* **580** (2006) 3167–3172.
24. Z. Kovarik, M. Čalić, G. Šinko, and A. Bosak, *Arh. Hig. Rada Toksikol.* **58** (2007) 201–209.
25. L. P. A. De Jong, M. A. A. Verhagen, J. P. Langenberg, I. Hagedorn, and M. Löffler, *Biochem. Pharmacol.* **38** (1989) 633–640.
26. F. Worek, H. Thiermann, L. Szinicz, and P. Eyer, *Biochem. Pharmacol.* **68** (2004) 2237–2248.
27. E. Heilbronn, *Biochem. Pharmacol.* **12** (1963) 25–36.
28. C. Luo, A. Saxena, Y. Ashani, H. Leader, Z. Radić, P. Taylor, and B. P. Doctor, *Chem.-Biol. Interact.* **119–120** (1999) 129–135.
29. Y. Ashani, A. K. Bhattacharjee, H. Leader, A. Saxena, and B. P. Doctor, *Biochem. Pharmacol.* **66** (2003) 191–202.
30. L. Francisković, M. Škrinjarić-Špoljar, and E. Reiner, *Chem.-Biol. Interact.* **87** (1993) 323–328.
31. K. Kuča, J. Patočka, and J. Cabal, *J. Appl. Biomed.* **1** (2003) 207–211.
32. R. Odžak, M. Čalić, T. Hrenar, I. Primožič, and Z. Kovarik, *Toxicology* **233** (2006) 85–96.
33. Y.-P. Pang, T. M. Kollmeyer, F. Hong, J. Lee, P. I. Hammond, S. P. Haugabouk, and S. Brimijoin, *Chem. Biol.* **10** (2003) 491–502.
34. F. Ekström, Y.-P. Pang, M. Boman, E. Artursson, C. Akfur, and S. Börjegen, *Biochem. Pharmacol.* **72** (2006) 597–607.
35. M. Škrinjarić-Špoljar, V. Simeon, E. Reiner, and B. Krauthacker, *Acta Pharm. Jugosl.* **38** (1988) 101–109.
36. Z. Kovarik, N. Ciban, Z. Radić, V. Simeon-Rudolf, and P. Taylor, *Biochem. Biophys. Res. Commun.* **342** (2006) 973–978.
37. A. Bosak, I. Primožič, M. Oršulić, S. Tomić, and V. Simeon-Rudolf, *Croat. Chem. Acta* **78** (2005) 121–128.
38. J. Patočka, J. Bajgar, and J. Bielavsky, *Collect. Czech. Chem. Commun.* **38** (1973) 3685–3693.
39. M. Škrinjarić-Špoljar, L. Francisković, Z. Radić, V. Simeon, and E. Reiner, *Acta Pharm.* **42** (1992) 77–83.
40. K. Sakurada, H. Ikegaya, H. Ohta, T. Akutsu, and T. Takatori, *Toxicol. Lett.* **166** (2006) 255–260.
41. V. Simeon, Z. Radić, and E. Reiner, *Croat. Chem. Acta* **54** (1981) 473–480.
42. E. Reiner, *Croat. Chem. Acta* **59** (1986) 925–931.
43. K. Kuča and J. Kassa, *J. Enzym. Inhib. Med. Chem.* **18** (2003) 529–535.

## SAŽETAK

### *In vitro* reakcije aldoksima i ljudske acetilkolinesteraze

**Zrinka Kovarik, Maja Čalić, Anita Bosak, Goran Šinko i Dubravko Jelić**

Proučavali smo reaktivaciju ljudske eritrocitne acetilkolinesteraze inhibirane tabunom, pri čemu smo povezali molekulske karakteristike jedanaest aldoksima s njihovim brzinama reaktivacije. Proveli smo konformacijsku analizu aldoksima primjenom molekulske mehanike kako bismo odredili savitljivost pojedinih aldoksima. Semiempirijski proračuni su pokazali da razlike u brzinama reaktivacije nisu posljedica različite elektronske gustoće na atomu kisika oksimske skupine, već mogu biti objašnjene steričkim smetnjama unutar same molekule. Učinkovita reaktivacija inhibirane acetilkolinesteraze postignuta je sa savitljivijim bispiridinijevim *para*-aldoksimima koji imaju propilensku ili butilensku poveznicu. Iako piridinijevi ili imidazolijevi aldoksimi s oksimskom skupinom u *ortho*-položaju nisu učinkovito reaktivirali fosforiliranu acetilkolinesterazu, oni su je štitili od fosforilacije tabunom zbog njihovog visokog afiniteta vezanja za nativnu acetilkolinesterazu. Ispitana je i citotoksičnost aldoksima za različite stanične linije. Citotoksični efekt aldoksima nije primijećen do njihove koncentracije od 400  $\mu\text{mol dm}^{-3}$ .